DOI: 10.1002/anie.201400653

Neurochemistry

Cytoskeletal Actin Dynamics are Involved in Pitch-Dependent Neurite Outgrowth on Bead Monolayers**

Kyungtae Kang, Seo Young Yoon, Sung-Eun Choi, Mi-Hee Kim, Matthew Park, Yoonkey Nam, Jin Seok Lee,* and Insung S. Choi**

Abstract: *Neurite outgrowth is an important preceding step for the development of nerve systems. Given that the in vivo environments of neurons consist of numerous hierarchical micro/nanotopographies, there have been many efforts to investigate the relationship between neuronal behaviors and surface topography. The acceleration of neurite outgrowth was recently reported on surfaces with a periodic nanotopography, but the biological mechanism has not yet been elucidated. In this work, the initial neurite development of hippocampal neurons on assembled silica beads with diameters ranging from 700 to 1800 nm was explored. The acceleration of neurite outgrowth increased with the surface-pitch size and leveled off after a pitch of 1 μm. Biochemical analysis indicated that cytoskeletal actin dynamics were primarily responsible for the recognition of surface topography. This work contributes to the emerging research field of topographical neurochemistry, as well as applied fields including neuroregeneration and neuroprosthetics.*

Neurites (axons and dendrites) are the cytoplasmic projections of neurons, and their direction, location, elongation, and even the time point of neuritogenesis directly determine the synaptic connections between neurons for the flow of information through the network. For the proper construction of the neural network, each neuron has the innate machinery to interpret the surrounding environment and determine the correct direction for sprouting neurites. Previous studies have shown that the specific recognition of biochemical cues is intimately connected with the local cytoskeletal dynamics at growth cones, the F-actin-based dynamic tips of neurites, during neurite outgrowth or guidance.[1–7] In addition to biochemical cues, there exists an often ignored but important environmental factor that also controls neuronal behaviors in vivo, namely "topography". The extracellular matrix (ECM) constructs the topographical environment for neurons and contains hierarchical micro/nanostructures composed of protein fibers (e.g., collagens and elastins) embedded with smaller fibril structures.[8]

The connection between neuronal behavior and micro/nanotopographical features has been investigated since contact guidance, which is the aligned growth or migration of cells to the physical shape of substrates, was demonstrated in neurons by using lithographically fabricated microgrooves.[9–11] The fabrication of nanostructures has allowed for the discovery of far more intriguing responses of neurons to nanotopographical cues;[12–21] most importantly, the acceleration of neuritogenesis. The developmental acceleration of neurites was initially reported on electrospun nanofibers,[20] and the presence of a threshold pitch for the acceleration effect was subsequently found on periodic nanostructures such as anodized aluminum oxide (AAO)[22] and assembled silica beads.[23,24] Although these reports strongly suggest that nanotopography is biologically recognized by neurons, the nature of the topographical influence on neuronal behaviors at the intracellular level remains elusive. With the consideration that both neurons and the ECM have heterogeneous, hierarchical structures, particularly at the submicro- and micrometer scales, we investigated the initial development of hippocampal neurons on topographical substrates in this range (pitch from approximately 700 to 1800 nm), and found that the acceleration of neurite outgrowth was saturated at pitches longer than 1000 nm. Biochemical analysis indicated that neuronal recognition of surface topography was governed by cytoskeletal actin.

Surfaces with various pitches were fabricated by organizing silica beads into two-dimensional, monolayer arrays on glass substrates (Figure S1 in the Supporting Information). Beads with diameters of 110, 320, 670, 1000, 1200, 1300, 1480, or 1750 nm were used in the study (SB-110, SB-320, SB-670, SB-1000, SB-1200, SB-1300, SB-1480, and SB-1750, respectively; with SB-110 as the control). Primary hippocampal neurons derived from E-18 Sprague Dawley rats were cultured on the closely packed bead layer (density of 50–200 cells/mm^2; Scheme 1). Before plating, each substrate with a different bead size was tailored to be neuron-adhesive by

[*] Dr. K. Kang,[+] M.-H. Kim, M. Park, Prof. Dr. I. S. Choi
Center for Cell-Encapsulation Research, Department of Chemistry
KAIST, Daejeon 305-701 (Korea)
E-mail: ischoi@kaist.ac.kr
Homepage: http://cisgroup.kaist.ac.kr
Dr. K. Kang,[+] Prof. Dr. Y. Nam, Prof. Dr. I. S. Choi
Department of Bio and Brain Engineering
KAIST, Daejeon 305-701 (Korea)
E-mail: ynam@kaist.ac.kr
Homepage: http://neuros.kaist.ac.kr
S. Y. Yoon,[+] S.-E. Choi, Prof. Dr. J. S. Lee
Department of Chemistry, Sookmyung Women's University
Seoul 140-742 (Korea)
E-mail: jinslee@sookmyung.ac.kr
Homepage: http://fetns.sookmyung.ac.kr
[+] These authors contributed equally to this work.

[**] This work was supported by the National Research Foundation of Korea (NRF) grant funded by the Korea government (MSIP) (2012R1A3A2026403, 2012R1A2A1A01007327, 2012-0009562, 2012R1A1A2022597, and 2012M3A7B4034986).

Supporting information for this article, including experimental details, is available on the WWW under http://dx.doi.org/10.1002/anie.201400653.

coating it with poly-D-lysine (PDL), preceded by O_2 plasma treatment. Neurons adhered and survived well on the bead layers with normal development of neurites and growth cones (Figure S2). The developmental behavior of the cultured neurons was analyzed at 1 day in vitro (DIV) in order to investigate the differences in the neuritogenesis phase. Since the beads made the substrates opaque, the cultured neurons were fixed and immunostained with anti-β-tubulin and phalloidin to target microtubules and F-actin, respectively.

The neuronal morphologies on the submicrometric pitches were remarkably different to those on the controls (coverslip and SB-110; Figure 1). At 1 DIV, the neurons on

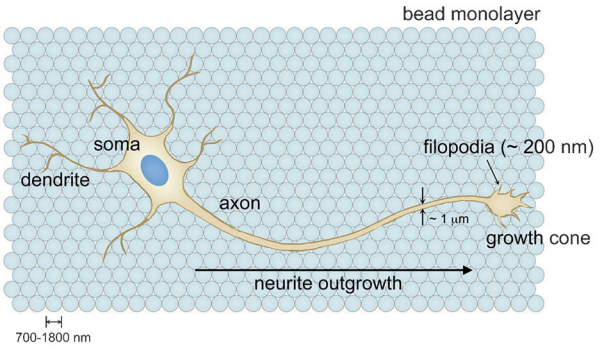

Scheme 1. Illustration of a neuron cultured on a silica-bead substrate.

the coverslip or SB-110 had barely sprouted neurites (red staining) and possessed the lamellipodial structures (green staining) that were generally found in the neuron culture on flat surfaces at 1 DIV (Figure 1a,b).[23] In stark contrast, the neurons on SB-670 had already developed the major neurite (a neurite more than double the length of the other neurites), and the formation of a growth cone and lateral filopodial structures was confirmed by the F-actin staining (Figure 1c). Lamellipodial structures surrounding the somas were not observed on SB-670 at 1 DIV. These morphological changes continued for the neurons on bigger beads (SB-1000, SB-1200, SB-1300, SB-1480, and SB-1750) but with significantly longer major neurites (Figure 1d,e and Figure S3). The averaged lengths of the longest neurite for each neuron clearly showed enhanced acceleration on the larger beads (Figure 1f): the length increased with the bead diameter (pitch; e.g., [SB-670: (52.46 ± 2.30) μm; SB-1000: (67.64 ± 4.90) μm]. Beyond SB-1000, however, there was no significant increase in neurite length with increasing bead diameter [SB-1200: (71.24 ± 7.51) μm; SB-1300: (74.93 ± 3.77) μm; SB-1480: (75.59 ± 4.81) μm; SB-1750: (69.09 ± 3.35) μm; there was no statistically significant difference between the values]. This result indicates that there was a saturation point or an upper threshold for the pitch dependency of accelerated neurite outgrowth. Developmental analysis of the neurons on selected bead substrates showed a similar trend of pitch dependency (Figure S4), thus implying that accelerated neuritogenesis contributed to the increased neurite length observed.

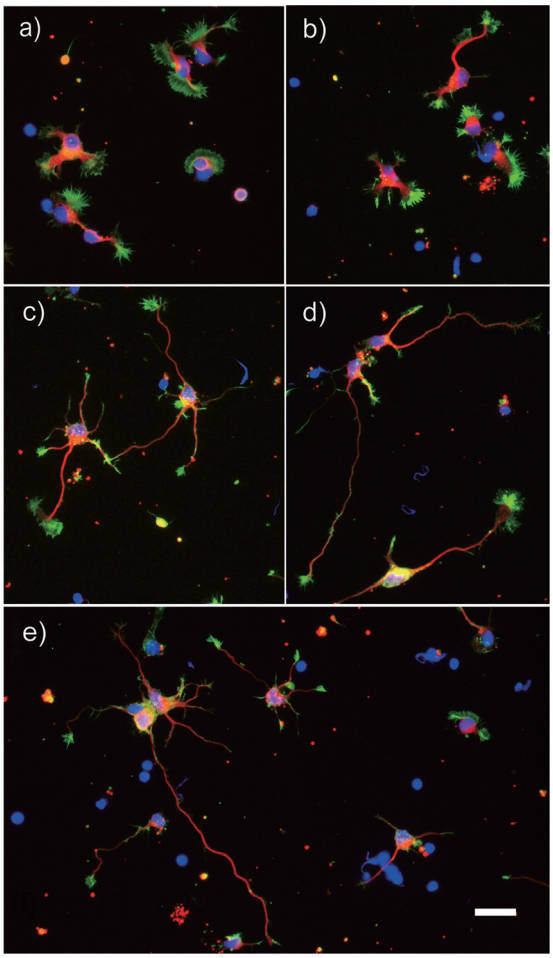

Figure 1. Fluorescence micrographs of hippocampal neurons at 1 DIV. The neurons were immunostained with anti-β-tubulin (red), phalloidin (green), and Hoechst 33342 (blue). The cells were cultured on a) Glass coverslip, b) SB-110, c) SB-670, d) SB-1000, and e) SB-1200. Scale bar: 25 μm. f) Average lengths (mean ± standard error) of the longest neurite on each substrate. All of the results were analyzed by one-way ANOVA at a significance level of 95%, followed by Bonferroni's multiple comparison test (N = 157, 114, 123, 117, 108, 113, 118, and 153 for coverslip, SB-110, SB-670, SB-1000, SB-1200, SB-1300, SB-1480, and SB-1750, respectively; $*P < 0.05$; $***P < 0.001$).

Notably, the acceleration effect was not intensified limitlessly as the pitch increased. The existence of an upper threshold found in this study complemented our previous report that showed the presence of a lower threshold of around 200–300 nm, a size comparable with the thickness of

the filopodia at the growth cone.[23] In the report, the filopodial activities were suggested to play a crucial role in the recognition of nanotopographical features at pitches of around 200 nm and above, thus implying a biological connection with the cytoskeletal dynamics of neurons. The upper threshold of 1000 nm (1 μm) would also have important biological implications because most individual axons are around 1 μm across.

The cytoskeletal dynamics at the growth cone, which are governed by actins and microtubules, are responsible for the rate and direction of neurite outgrowth, as well as the morphology of growth cones. Like the biochemical guidance cues that modulate cytoskeletal dynamics through guidance receptor signaling,[3,25–27] surface topographical features have also been reported to influence the cytoskeletal proteins of cells.[18,23,28] To gain insight into the biological mechanisms of topographical recognition by neurons, we used three different biochemical inhibitors of neuronal cytoskeletal dynamics (Figure 2a): cytochalasin D (inhibitor of the formation/function of F-actin), nocodazole (inhibitor of microtubule formation), and blebbistatin (inhibitor of nonmuscle myosin II). Blebbistatin was used to break the balance of F-actin dynamics by impeding retrograde F-actin flow. The topography-distinguishing ability of the neurons was lost completely upon treatment with cytochalasin D, nocodazole, or blebbistatin (Figure 2b,c). After treatment with cytochalasin D (1 μM), the neurites became elongated and thinner and multiple major neurites were frequently observed (Figure S5a,b), most likely because the absence of F-actin structures made the microtubules advance in an uncontrolled

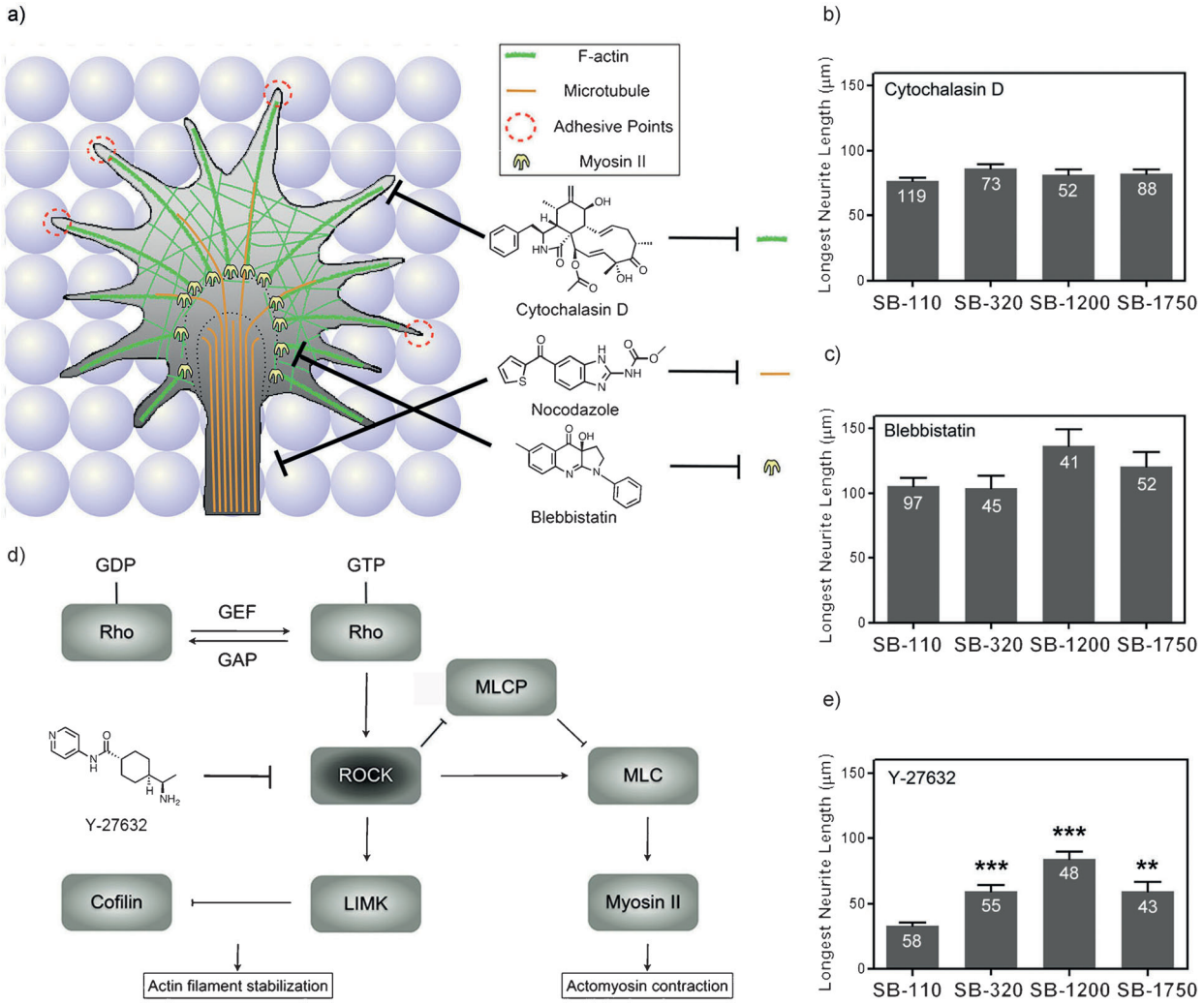

Figure 2. a) Illustration of a growth cone and the chemical structures of the biochemical inhibitors. b,c) Average lengths (mean ± standard error) of the longest neurite on each substrate treated with cytochalasin D (b) or blebbistatin (c). There were no significant differences between any pair in (b) and (c). A large portion of actin dynamics is known to be regulated by the Rho/ROCK pathway, which includes the Rho family of small GTPases and their downstream effectors. The Rho/ROCK pathway normally starts with the biochemical activation of G-protein-coupled receptors (GPCRs), and its downstream function enhances actin dynamics by simultaneously stabilizing actin filaments and generating actomyosin contraction forces. d) Diagram showing the Rho/ROCK pathway for cytoskeletal dynamics. MLC = myosin regulatory light chain; MLCP = myosin regulatory light chain phosphatase; LIMK = LIM kinase. e) Average lengths (mean ± standard error) of the longest neurite on each substrate after treatment with Y-27632. The substrates were compared to SB-110 by one-way ANOVA at a significant level of 95%, followed by Bonferroni's multiple comparison test (**$P < 0.01$; ***$P < 0.001$). The numbers indicate the number of data points for statistics.

fashion. The lengths of the major neurites were in the range of 76–86 μm and no statistically significant differences were found between the various pitches, thus indicating the importance of actin dynamics in pitch-dependent neurite outgrowth (Figure 2b; Figure S6a). In the case of nocodazole (100 nM), the neurons barely developed neurites on any of the substrates owing to the impeded formation of microtubules (data not shown). Blebbistatin treatment (25 μM) caused similar neuronal morphology to cytochalasin D, but with more elongated (103–137 μm) F-actin bundles (Figure 2c; Figure S5c,d and Figure S6b). These results indicate that actin dynamics, and not simply the presence of F-actin, were responsible for the topographical recognition. It is to be emphasized that the inhibitor treatment led to neurite elongation in an uncontrolled manner to give abnormal neuronal morphologies; by contrast, the topographical cues provided by the silica beads maintained the normal development of neurons with accelerated neurite outgrowth. Therefore, it is plausible that the neurons recognize surface topography and induce dramatic changes of intracellular actin dynamics in a biologically controlled, organized fashion for the acceleration of neurite outgrowth. Because the Rho/ROCK pathway is a well-established pathway involved in the regulation of actin cytoskeletal proteins (Figure 2d),[29] we investigated the effect of Y-27632, a selective inhibitor of ROCK, on the neuronal recognition of surface topography. In contrast to the biochemical inhibitors, neurons treated with Y-27632 (10 μM) retained their topography-distinguishing ability (Figure 2e), with remarkable neurite elongation on SB-1200 compared with the other substrates (Figure S6c). By contrast, on coverslips (the control), Y-27632 treatment caused dose-dependent neurite elongation (Figure S7). This implies that biophysical cues (topography) may induce intracellular pathways other than the Rho/ROCK pathway to influence neuritogenesis and neurite outgrowth.[30]

In summary, we report the possible existence of an upper pitch threshold for the accelerated neurite outgrowth of primary hippocampal neurons on bead monolayers. The fact that the lower and upper ranges of pitches that affect acceleration ($\approx$200 nm and 1 μm) correspond to the sizes of filopodia at growth cones and typical axons, respectively, is certainly intriguing. Mechanistic studies with biochemical inhibitors indicated that F-actin dynamics generated by myosin II were involved in the recognition of the surface topography. One possible mechanism involves tension-based acceleration of neurite outgrowth (Figure 3).[31,32] As the distance between contact points increases, the suspended mass of the neurite ($\lambda_m l$) increases as well. The pull of gravity on this increased mass generates more tension, which may stimulate accelerated outgrowth. Beyond a certain length, however, neurites may follow the curvature of the substrate rather than suspend additional mass, and this places an upper limit on the possible amount of tension generated. However, more detailed studies are needed to fully elucidate the role of localized tension in the neuronal recognition of surface topography. In addition, the existence of mechanoreceptors in hippocampal neurons also remains to be demonstrated.

Recent reports clearly showed a biological connection between environmental topographical features at nano- and submicrometer scales and neuritogenesis and the morphogenesis of neurons.[18–23] This report on the upper threshold provides crucial information for the emerging research field of topographical neurochemistry, as well as for practical applications such as neuroregeneration and neuroprosthetics.

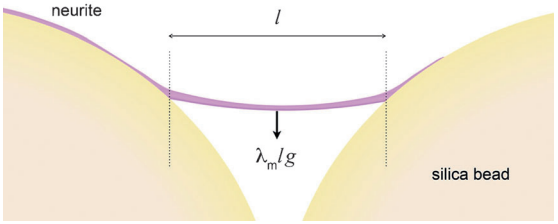

Figure 3. Illustration of a neurite on a beaded surface. Physical tension arises from the gravitational force exerted on the neurite portion hanging between the beads (length: l). λ_m = linear mass density; g = gravitational acceleration constant. Not drawn to scale.

Experimental Section

Cell Culture: Primary hippocampal neurons were cultured in serum-free conditions. Hippocampus from E-18 Sprague Dawley rat was triturated in 1 mL of Hank's Balanced Salt Solution (HBSS) by using a fire-polished Pasteur pipette. The cell suspension was centrifuged for 2 min at 1000 rpm, and a cell pellet was extracted. The cell pellet was suspended in Neurobasal media supplemented with B-27, L-glutamine (2 mM), L-glutamic acid (12.5 μM), and penicillin/streptomycin. Dissociated cells were seeded at a density of 50–200 cells/mm^2 on a silica nanobead substrate. Cultures were maintained in an incubator (5% CO_2 and 37°C), and half of the medium was replaced with fresh culture media without L-glutamic acid supplement every 3–4 days. This study was approved by IACUC (Institutional Animal Care and Use Committee) of KAIST.

Instruments and Characterizations: The surface topography of the prepared substrates was investigated by field-emission scanning electron microscopy (FE-SEM; Hitachi S-4800). Before FE-SEM imaging, the cultured substrates were coated with platinum (30 mA, 360 s). Fluorescence micrographs of neuron cultures were obtained by using an Olympus BX51M (Olympus) equipped with a CCD camera (DP71, Olympus). From the images, the lengths of major neurites were measured with the Neuron J plugin in Image J software (NIH).

Received: January 21, 2014
Published online: March 5, 2014

Keywords: axon outgrowth · cytoskeletal proteins · nanostructures · neurochemistry · silica beads

[1] B. J. Dickson, *Science* **2002**, *298*, 1959–1964.
[2] E. W. Dent, F. B. Gertler, *Neuron* **2003**, *40*, 209–227.
[3] J. S. da Silva, C. G. Dotti, *Nat. Rev. Neurosci.* **2002**, *3*, 694–704.
[4] E. W. Dent, S. L. Gupton, F. B. Gertler, *Cold Spring Harbor Perspect. Biol.* **2011**, *3*, a001800.
[5] F. Bradke, *Science* **1999**, *283*, 1931–1934.
[6] P. K. Mattila, P. Lappalainen, *Nat. Rev. Mol. Cell Biol.* **2008**, *9*, 446–454.
[7] L. Luo, *Nat. Rev. Neurosci.* **2000**, *1*, 173–180.
[8] a) M.-H. Kim, M. Park, K. Kang, I. S. Choi, *Biomater. Sci.* **2014**, *2*, 148–155; b) K. Kang, M.-H. Kim, M. Park, I. S. Choi, *J. Nanosci. Nanotechnol.* **2014**, *14*, 513–521.

[9] P. Clark, P. Connolly, A. S. Curtis, J. A. Dow, C. D. Wilkinson, *Development* **1987**, *99*, 439 – 448.
[10] A. M. Rajnicek, C. D. McCaig, *J. Cell Sci.* **1997**, *110*, 2915 – 2924.
[11] A. M. Rajnicek, S. Britland, C. D. McCaig, *J. Cell Sci.* **1997**, *110*, 2905 – 2913.
[12] S. P. Khan, G. G. Auner, G. M. Newaz, *Nanomedicine* **2005**, *1*, 125 – 129.
[13] V. Brunetti, G. Maiorano, L. Rizzello, B. Sorce, S. Sabella, R. Cingolani, P. P. Pompa, *Proc. Natl. Acad. Sci. USA* **2010**, *107*, 6264 – 6269.
[14] F. Johansson, M. Kanje, C. E. Linsmeier, L. Wallman, *IEEE Trans. Biomed. Eng.* **2008**, *55*, 1447 – 1449.
[15] W. Hällström, T. Mårtensson, C. Prinz, P. Gustavsson, L. Montelius, L. Samuelson, M. Kanje, *Nano Lett.* **2007**, *7*, 2960 – 2965.
[16] C. Xie, L. Hanson, W. Xie, Z. Lin, B. Cui, Y. Cui, *Nano Lett.* **2010**, *10*, 4020 – 4024.
[17] A. Ferrari, M. Cecchini, A. Dhawan, S. Micera, I. Tonazzini, R. Stabile, D. Pisignano, F. Beltram, *Nano Lett.* **2011**, *11*, 505 – 511.
[18] K.-J. Jang, M. S. Kim, D. Feltrin, N. L. Jeon, K.-Y. Suh, O. Pertz, *PLoS One* **2010**, *5*, e15966.
[19] H. S. Koh, T. Yong, C. K. Chan, S. Ramakrishna, *Biomaterials* **2008**, *29*, 3574 – 3582.
[20] C. C. Gertz, M. K. Leach, L. K. Birrell, D. C. Martin, E. L. Feldman, J. M. Corey, *Dev. Neurobiol.* **2010**, *70*, 589 – 603.
[21] J. Xie, M. R. MacEwan, X. Li, S. E. Sakiyama-Elbert, Y. Xia, *ACS Nano* **2009**, *3*, 1151 – 1159.
[22] W. K. Cho, K. Kang, G. Kang, M. J. Jang, Y. Nam, I. S. Choi, *Angew. Chem.* **2010**, *122*, 10312 – 10316; *Angew. Chem. Int. Ed.* **2010**, *49*, 10114 – 10118.
[23] K. Kang, S.-E. Choi, H. S. Jang, W. K. Cho, Y. Nam, I. S. Choi, J. S. Lee, *Angew. Chem.* **2012**, *124*, 2909 – 2912; *Angew. Chem. Int. Ed.* **2012**, *51*, 2855 – 2858.
[24] J. S. Lee, J. H. Kim, Y. J. Lee, N. C. Jeong, K. B. Yoon, *Angew. Chem.* **2007**, *119*, 3147 – 3150; *Angew. Chem. Int. Ed.* **2007**, *46*, 3087 – 3090.
[25] N. Arimura, K. Kaibuchi, *Neuron* **2005**, *48*, 881 – 884.
[26] C. Gonzalez-Billault, P. Muñoz-Llancao, D. R. Henriquez, J. Wojnacki, C. Conde, A. Caceres, *Cytoskeleton* **2012**, *69*, 464 – 485.
[27] I. de Curtis, J. Meldolesi, *J. Cell Sci.* **2012**, *125*, 4435 – 4444.
[28] J. Albuschies, V. Vogel, *Sci. Rep.* **2013**, *3*, 1658.
[29] a) C. D. Nobes, A. Hall, *Cell* **1995**, *81*, 53 – 62; b) M. Lehmann, A. Fournier, I. Selles-Navarro, P. Dergham, A. Sebok, N. Leclerc, G. Tigyi, L. McKerracher, *J. Neurosci.* **1999**, *19*, 7537 – 7547.
[30] T. L. Downing, J. Soto, C. Morez, T. Houssin, A. Fritz, F. Yuan, J. Chu, S. Patel, D. V. Schaffer, S. Li, *Nat. Mater.* **2013**, *12*, 1154 – 1162.
[31] S. Chada, P. Lamoureux, R. E. Buxbaum, S. R. Heidemann, *J. Cell Sci.* **1997**, *110*, 1179 – 1186.
[32] C. C. DuFort, M. J. Paszek, V. M. Weaver, *Nat. Rev. Mol. Cell Biol.* **2011**, *12*, 308 – 319.

